Splashing of Sn-Bi-Ag solder droplets

K. L. Meza-Alarcon,[1] M. A. Quetzeri-Santiago,[2] M. A. Neri-Flores,[3] J. Antonio del Río,[4, a)] and J. R. Castrejón-Pita[5]

[1)]*School of Engineering and Material Sciences, Queen Mary University of London, E1 4NS, United Kingdom.*

[2)]*Department of Engineering Science, University of Oxford, Oxford OX1 3PJ, UK*

[3)]*Centro de Investigación en Materiales Avanzados, Miguel de Cervantes 120, Complejo Ind., Chihuahua, México*

[4)]*School of Engineering and Material Sciences, Queen Mary University of London, E1 4NS, United Kingdom.*

[5)]*Department of Mechanical Engineering, University College London, Torrington Place, London WC1E 7JE, United Kingdom*

(Dated: 28 July 2023)

In this paper, we study the behaviour and spreading dynamics of molten metallic alloy droplets. Five solders, including three rare earths and a commercial alloy, were used to assess their splashing behaviour in terms of the material and impacting conditions. The metallic solders were melted down in a heated chamber (oven) and then dripped onto a smooth copper flat substrate as spherical droplets. The impact of each alloy droplet was recorded and analysed by high-speed imaging and image analysis to obtain the impact speed, the droplet size and the dynamic contact angle. Our results show that the impact behaviour is well parameterised by the splashing ratio, a dimensionless number encompassing the impact and liquid properties, and the maximum dynamic spreading contact angle. Our results are useful to the industry as they provide a criterion to select the maximum soldering injection speed, or the droplet size, to avoid splashing during soldering or the jetting of molten metals.

[a)]On sabbatical leave from Instituto de Energias Renovables, Universidad National Autónoma de México, 62580 Temixco, Morelos México.

I. INTRODUCTION

The era of the internet-of-things has brought the ubiquity of electronic devices and sensors to our daily life at a time when the world fights to become more sustainable. Substantial efforts by the digital industry are focused on improving the already efficient manufacturing methods and the development of green electronic materials and components. In particular, the printing of electronics is a very active area of research that aims to bring the benefits of inkjet methods to the manufacturing of electronic devices[1]. Inkjet uses liquid droplets to create patterns on a variety of substrates, including fabrics, ceramics, and paper. Inkjet is additive and digital, so it neither produces waste nor requires a template. Recent advances permit the printing of inks containing metallic particles and conductive polymers for the manufacturing of electric tracks and simple circuits. Current studies in inkjet systems aim to improve resolution by improving the jetting and impact of droplets. Other challenges remain in the field, such as the direct jetting of metals or the printing of high viscosity liquids.

Droplet impact has been widely studied since the pioneering work of Worthington at the start of the 20th century[2]. Since then, multiple studies have focused on understanding the impacting behaviour of droplets, that range from smooth deposition and spreading, to bouncing and splashing[3,4]. Past works have demonstrated that the impact behaviour depends on the liquid properties (surface tension γ, and density ρ)[5–7], the substrate properties (roughness, curvature, wettability and stiffness)[8–12], the ambient gas[13–15], and the droplet size and speed (D_0 and U_0, respectively)[3]. At slow impacting velocities, a droplet smoothly spreads over a substrate to reach a maximum diameter to then recede to an equilibrium state. Faster impacts trigger the growth of surface instabilities that form finger-shaped structures at the spreading rim (often called lamella)[4]. Above a critical impacting speed, these instabilities break up the rim generating secondary droplets; this is defined as splashing[3,4].

The impact of droplets has been studied in terms of various scaling parameters such as the Weber number, the splashing parameter, and the capillary number[5,16]. For example, the Weber number (We = $\rho D_0 U_0^2/\gamma$) has been used to characterise droplet impact on liquid surfaces at different temperatures[17], and to study the simultaneous impact of droplets on molten surfaces[18]. While these dimensionless numbers can successfully parametrise the impact behaviour of a single liquid-substrate system, only the splashing ratio and the dynamic contact angle have been proven to divide the splashing/no-splashing behaviour across multiple substrates and liquids,[11]. The splashing

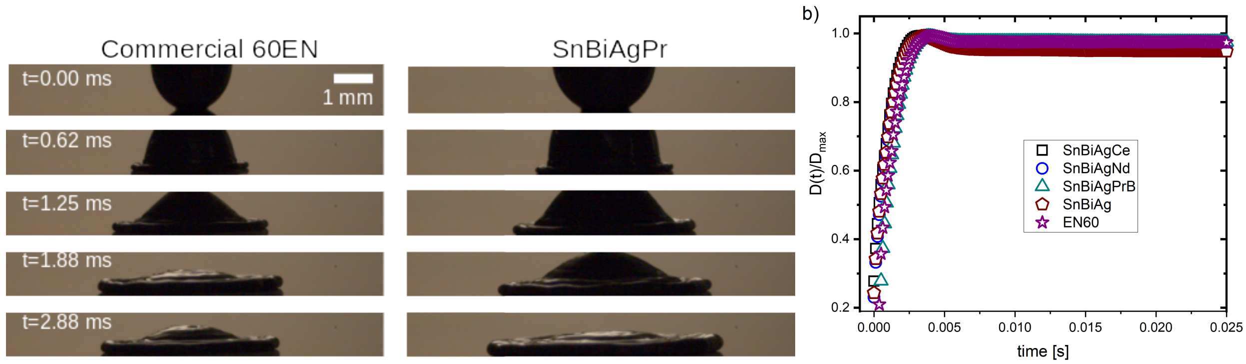

FIG. 1. Impact and spreading dynamics of molten metal alloys on a flat copper plate at room temperature (22 Celsius). a) Experimental snapshots at different times, taken by high-speed imaging at 8,000 fps. b) Dimensionless spreading diameter, $D(t)/D_{max}$, in terms of time from impact. All alloys recede after reaching the maximum spreading diameter D_{max}, solidification occurs at much later times.

ratio is given by $\beta \approx 1.73 \frac{\mu_g^{1/2}(\rho D_0)^{1/6} U_0^{5/6}}{\gamma^{2/3}}$, where μ_g is the ambient gas viscosity, and represents the balance between surface tension and the aerodynamic forces acting on the spreading lamella. Splashing occurs above a critical point, where aerodynamic forces dominate surface tension breaking up the lamella. Indeed, droplet splashing on rough and smooth flat substrates has been found to be correctly parameterised by the splashing ratio and the contact angle for various liquids on surfaces ranging from hydrophilic to superhydrophobic[11,14,19].

In addition to the standard liquid properties, in molten metals, the substrate temperature and the thermal properties has been found to play a role in splashing. Aziz and Chandra, in 1999[20], studied the impact of tin droplets on steel at room and above-melting temperatures. They observed a more prominent splashing on heated surfaces than those at room temperature; solidification arresting breakup[20]. Gielen et al., in 2020, found that the critical splashing velocity of molten metal drops depends on the substrate temperature[21]. In contrast, Dhiman and Chandra, in 2005[22], found that tin droplets splash on cold aluminium and stainless steel surfaces but do not splash on hot surfaces. They argued that droplet solidification near the contact line triggers instabilities that lead to splashing[22]. In fact, in molten tin, a sub-micron surface roughness triggers splashing but a micrometer-sized roughness prevents splashing due to changes in the solidification rate[23]. Additionally, other studies have demonstrated that heat transfer overcomes both surface tension and roughness on the splashing of gold droplets[24].

During the fabrication of electronic devices, molten metal droplets are used for the creation of solder bumps to connect chips and other electronics to a circuit board[25,26]. As part of the process, splashing is often observed[27]. Therefore, understanding the underlying mechanisms of droplet splashing are crucial when optimising the quality and efficiency of electric soldering. Sn-Pb-based solders have long been used by the worldwide electronics industry thanks to their excellent properties and characteristics, such as their low melting point ($\sim$ 180 Celsius), good wettability, and low price[28]. However, lead is toxic and a well-known contaminant of both soil and subsoil; eliminating lead from solders and electronics is highly desired. Sb-Ag-Cu alloys are widely used as lead-free solders, but their high-temperature melting point ($\sim$ 220 Celsius) can damage miniaturised electronic devices, such as those found within cell phones, smart watches and headphones. Other alternatives are the Sn-Bi-Ag-X alloys, where X stands for rare earth elements such as Cerium (Ce), Neodymium (Nd), and Praseodymium (Pr). These lead-free rare earth solders have a low melting point[29] ($<$ 139 Celsius, as seen in Table I) and readily satisfy current safety regulations in Europe and America[30]. In fact, earth elements in Sn-Bi-Ag improve the physical and mechanical properties of solders, making them the preferred choice for electronic device fabrication[31].

TABLE I. Physical properties of the alloys used in this work.

Alloy	Eq. contact angle	Density $\times 10^3$ kg/m^3	Surface tension mN/m	Melting T Celsius
SnBiAg	129±3	8.31	515 ±8	139.5
SnBiAgCe	117±3	8.51	585 ±8	136.8
SnBiAgPr	117±3	8.74	588 ±8	138.4
SnBiAgNd	129±3	8.47	634 ±2	138.5
60EN[32]	139±3	8.50	594	183.0

In this paper, we study the spreading and splashing dynamics of solder alloys containing Sn-Bi-Ag and rare earths, namely, Ce, Nd and Pr. The following alloy compositions, chosen to be near their eutectic points, were used: Sn-Bi-Ag 58.53%, 40.80%, 0.65%; Sn-Bi-Ag-Ce 62.74%, 36.3%, 0.66%, 0.18%; Sn-Bi-Ag-Nd 59.38%, 39.73%, 0.71%, 0.17%; Sn-Bi-Ag-Pr 61.83%, 37.14%, 0.69%, 0.32%. These alloys were characterised by Inductively Coupled Plasma Emission Spectrometry. Our results indicate that the liquid properties of these alloys (when molten) are similar to that of a commercial solder (60EN). As seen in Table 1, the alloys studied here have a similar density, surface tension and equilibrium contact angle than their commercial counterpart. How-

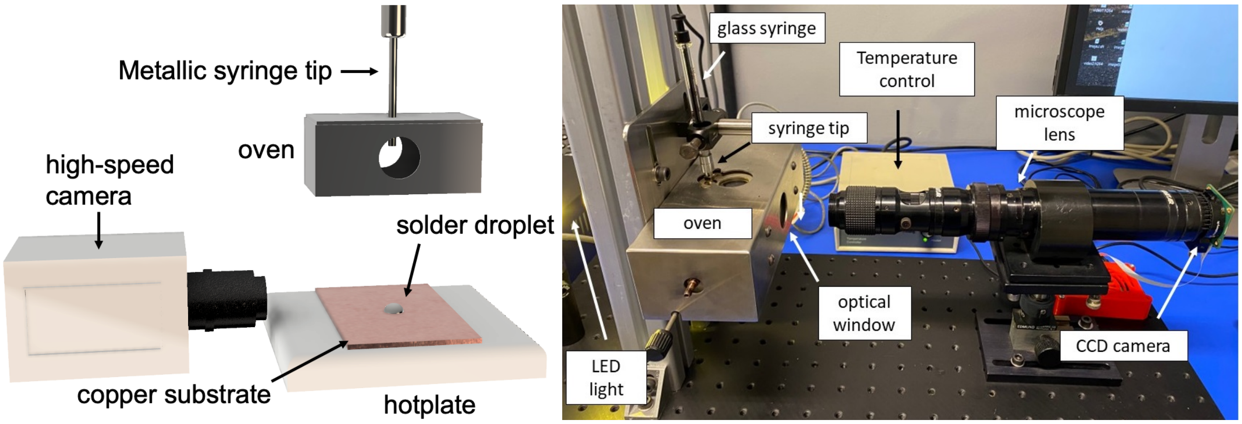

FIG. 2. (left) Schematic view of the experimental setup (not to scale). A pre-loaded syringe tip is heated in the oven to 220 °C where the alloy melts to form and drip a droplet. Droplet impacts are then recorded by high-speed imaging. (right) Experimental system used for the measurement of the (equilibrium) surface tension of pending droplets. The temperature within the oven is kept constant by a heating element and a thermometer found within the oven enclosure

ever, the Sn-Bi-Ag base is near its eutectic point so the resulting melting temperatures of the rare earth alloys are substantially better than the commercial one[31]. As describe above, these melting temperatures not only favour the soldering of small electrical elements but also had the additional benefits of energy saving. In addition, Cerium was used as its properties are close to that of Nd and Pr, but at a low cost. Interestingly, we found that a Neodymium doping significantly increases the alloy's equilibrium surface tension without affecting: wetting, the impact dynamics or the melting temperature. Furthermore, for the first time, we have obtained the dynamic wetting of these alloy's, through the measurement of the dynamic contact angle at spreading speeds up to 2.0 m/s. These results demonstrate that molten metal droplets acquire an asymptotic maximum contact angle during spreading. In addition, we found that the splashing behaviour of these alloys is correctly parameterised by the splashing ratio and the dynamic contact angle. In this letter, splashing is identified visually from experiments and defined as the event where the front of the impacting and spreading droplet breaks up into smaller droplets.

II. PRODUCING SOLDER DROPLETS

In this work, we use high-speed imaging to study the impact of the molten alloy droplets; the setup is illustrated in Fig. 2. In brief, the experiment consists of an oven mounted on a support, a flat copper substrate, a heated bed, and a high-speed camera. The oven is a metallic enclosure

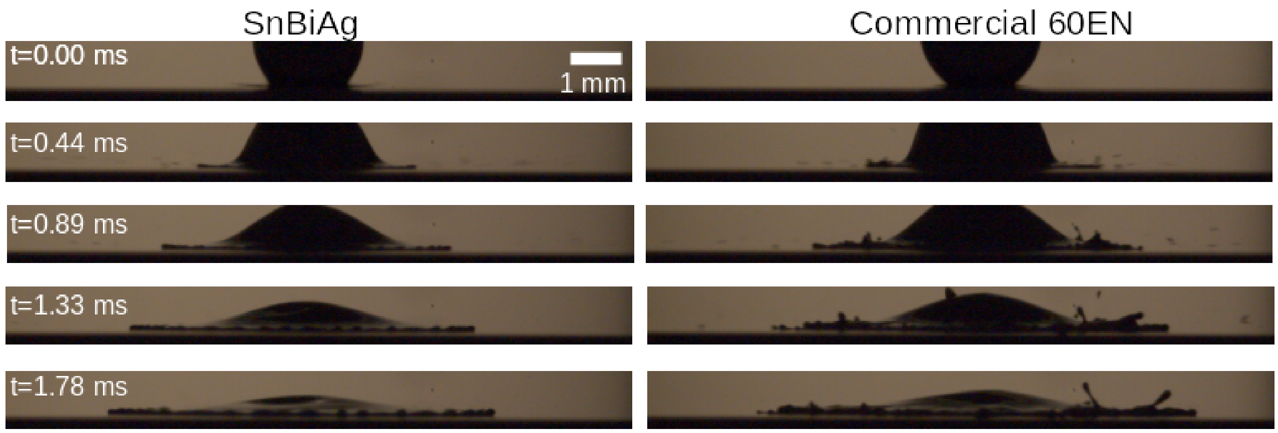

FIG. 3. Spreading and splashing dynamics of solder droplets impacting at 3.2 m/s a flat copper substrate at 22 Celsius. Secondary/satellite droplets detach from both the Sn-Bi-Ag and the (commercial solder) 60EN droplets at t = 0.44 ms. At later times (t = 0.89 - 1.78 ms), other secondary droplets detached from the 60EN droplet.

in which an electrical resistance heater, and a thermometer, control the inside conditions from room temperature to 220 Celsius. The enclosure has two circular apertures at the upper and lower sides; the upper orifice is used to introduce the metallic tip of a glass syringe that has been pre-loaded with the solder sample. The lower orifice permits a dripping droplet to exit the enclosure and impact the substrate below. The enclosure also has two optical windows on the side walls to observe the melting, formation and dripping of the metallic liquid droplets. Solder droplets are generated by heating the sample within the syringe tip to a temperature of 220 Celsius. After melting, the molten material is pushed through the syringe to slowly form a pendant drop at the tip. At this point, surface tension is measured using the pendant drop method and ImageJ[33]; the experimental setup is seen in Fig. 2. Surface tensions obtained by this method are found in Table I; densities were obtained by the Archimedes's method. After overhanging, the droplet is slowly pushed to detach from the tip and fall by gravity. Here, the droplet diameter was maintained approximately constant at $D_0 = 2.1 \pm 0.1$ mm. The falling distance was varied from 70 to 530 mm, leading to impacting velocities in the range of $U_0 = 0.97$-3.22 m/s. Our experiments were carried out in the low Ohnesorge number regime, Oh $\ll 1$, where Oh$= \mu/\sqrt{\rho\gamma D_0}$ and μ is the molten solder viscosity. In this range, according to Riboux and Gordillo in 2014 and de Goede et al. in 2018, liquid viscosity effects can be disregarded[14].

Experiments were conducted in air and at atmospheric pressure. In industrial and scientific

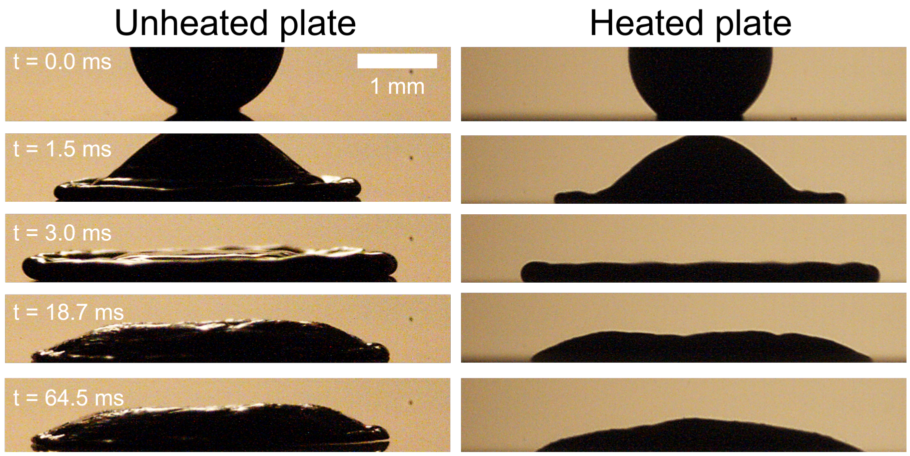

FIG. 4. Spreading dynamics of Sn-Bi-Ag-Pr droplets impacting at 1.0 m/s on a flat copper substrate at 22 Celsius (left), and 220 Celsius (right). As seen, the spreading dynamics see important differences at the region around the contact line after 3.0 ms. Solidification shows discernible effects; at 22 Celsius the contact line is pinned to the substrate and arrests receding. In contrast, at 220 Celsius, the droplet remains liquid, not pinned, and receding.

applications, soldering occurs under various environmental conditions ranging from standard atmospheric conditions to inert gas mediums[21,34]. Here, we decided to perform our experiments in air, as this condition is commonly found in industry and during standard prototyping. In fact, inert environments are often prohibitively costly to industries. Past works have studied the role of oxidation on the dynamics of liquid metals finding that oxide affects the breakup of liquid metal sheets[34]. Furthermore, Xu et al. in 2013 and Yang et al. in 2023 explored the effect of oxide on the impact dynamics of aluminium and gallium-indium droplets finding that viscous dissipation due to the oxide is negligible during spreading[35,36]. We note that our surface tension measurements, reported in Table 1, are in agreement with those taken within an inert atmosphere, i.e. Gielen et. al in 2020[21]. Our compelling parametrisation suggests that oxidation, or other effects acting on the contact line, are correctly captured by changes on the contact angle. Indeed, an interesting proposal for future work would be to study the effect of oxidation on the contact angle. Droplet impact was recorded at 8,000 fps at an exposure time of 17 μs. A Chronos camera and a 6$\times$ Navitar microscope lens were used at a resolution of 9.47 μm per pixel. All droplets impacted a copper plate set either at room temperature (22 Celsius) or at 250 Celsius. Dynamic and equilibrium contact angles were obtained by a custom-developed image analysis in Matlab[37]. In brief, the method detects and fits a second-order polynomial to the droplet boundary around the contact line, examples of the contact angle measurements in terms of the contact line velocity u_{cl} and time are shown in Fig. 5. Droplet sizes and impacting speeds were also determined from the image analysis in Matlab. The measurement of the contact angle is affected by resolution, the interrogation area, the polynomial fitting, and vertical offsets of the substrate,[37]. Here, we used a second-order polynomial fitting on a fitting domain equivalent to 4% of the droplet profile length produce the most accurate results. Under these conditions, we obtained our reported error on the dynamic contact angle, i.e. $\pm$ 3 degrees.

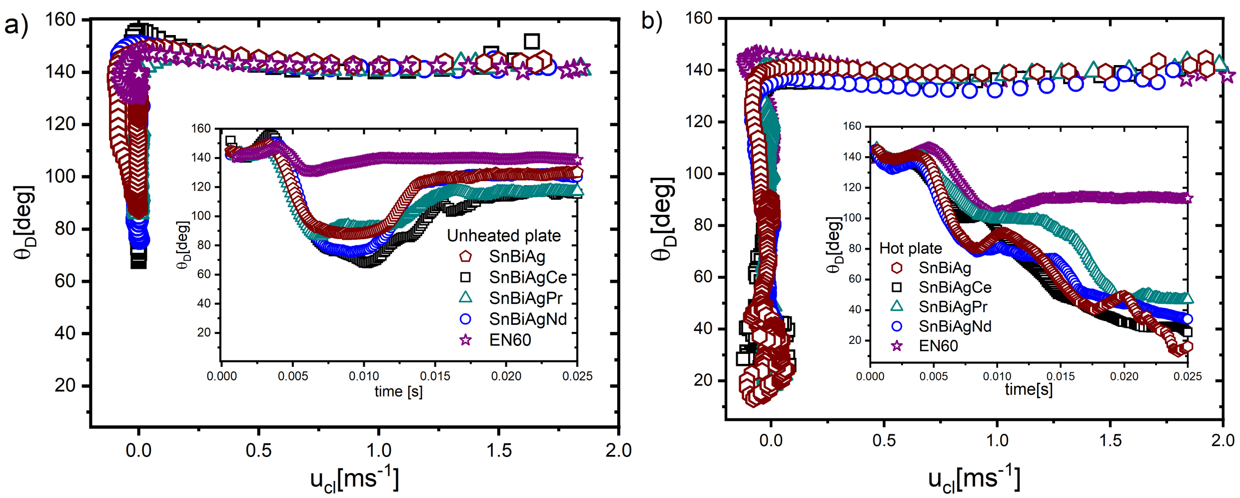

FIG. 5. Dynamic contact angle in terms of the contact line velocity u_{cl} of solder alloys impacting on a copper plate at a) 22 Celsius, and b) 250 Celsius. As seen, all the alloys spread at a constant contact angle. Insets show the dynamic contact angle in terms of the time from impact, where the differences between the unheated and heated impacts are much visible at $t \geq 0.15$ ms. Unheated droplets reach the equilibrium contact angle as they solidify. In contrast, in a heated impact, the contact angle oscillates and varies to gradually achieve equilibrium.

III. DYNAMICS OF A METAL DROPLET IMPACTING ON A RIGID PLATE

Figures 1 and 3 illustrate our results; a droplet impacting at $U_0 = 0.95$ m/s undergoes a smooth deposition and spreading (no splashing) but an impact at a higher speed ($U_0 = 3.2$ m/s) leads to splashing. During spreading ($t < 3$ ms), and within error bars, the dynamic contact angle of all the alloys takes an asymptotic constant value, often called the maximum dynamic spreading contact angle. For all alloys, $\theta_{max} = 145 \pm 3$ degrees, as seen in Figs. 1b and 5a. These results are consistent with the advancing contact angle measurements made by Aziz & Chandra in 2000 on tin droplets[20]. The spreading behaviour of the alloys and the commercial 60EN are found in Figure 1a. At early times ($t < 3$ ms), we see the droplets spreading to reach a maximum diameter and they acquire a pancake-like shape. In fact, at these times, the impact ($t \lesssim 3$ ms) and spreading dynamics are similar between alloys, regardless of the substrate temperature, indicating that, at such time scales, there is no phase transition (solidification); please also see Fig. 1 in the supplemental material. At longer times, for the impact at room temperature, we see the contact line receding to a stop due to solidification at $t = 5$ ms, as shown in Fig.1. In contrasts, the contact line remains mobile for longer times at the hot substrate; pinning is only observed at $t = 30$ ms, see Fig. 1 in the supplementary material. As demonstrated by Ruiter et al. in 2018[38], a spreading and freezing droplet follows a tank-treading like motion, where fresh liquid metal comes in contact with the substrate. In our experiments, Figure 4, we observed a mobile contact line during spreading and our advancing contact angle measurements correspond to that formed by the molten metal and the copper substrate. On heated substrates, the solder droplet remains liquid and free to recede, as seen in Figure 4.

The contact angle dynamics are found in Figs. 5a and b, where we see that, beyond spreading, the behaviour between impacting temperatures is different. For rare earth solders impacting the substrate at 22 Celsius, the contact line gets pinned 5 ms after impact, and the contact angle remains constant for about 10 ms at ~ 90 degrees. The contact angle then increases to take its equilibrium value 15 ms after impact as the droplet solidifies. In contrast, when impacting a substrate at 250 Celsius it does not experience solidification, and both the contact line and the contact angle remain mobile. In fact, the contact angle decreases gradually to reach an equilibrium tenths of milliseconds after impact. The dynamics of the 60EN commercial solder are different as the contact line pins earlier than its rare earth counterparts. Indeed, for both unheated and heated substrates, the contact angle dynamics of 60EN stops within the first 10 ms as a consequence of its higher melting temperature and a possible phase transition.

The splashing behaviour also shows differences in terms of the temperature of the substrate. Impacting at 2.0 m/s on a plate at room temperature results in splashing on all the alloys. Figure 3, shows the splashing of SnBiAg and 60EN droplets impacting the copper substrate at 3.2 m/s. As noted by past works[11,19], the splashing behaviour of Newtonian fluids, that are found in a natural liquid form at room temperature, has been well-parameterised by the splashing ratio β and the asymptotic dynamic contact angle θ_{max}. Accordingly, Figure 6 shows all the impacting experiments classified by their splashing behaviour, in terms of β and θ_{max}. As observed, the behaviour is well divided into two groups: droplets that impact and spread (no splashing, solid symbols) and droplets that impact and splash (hollow symbols). Indeed, a common critical splashing ratio, or spreading threshold, is found at $\beta \approx 0.0165$; the threshold common to both the impact on heated and the unheated substrates. A divide also exists between the dynamics at the two surface temperatures, the maximum spreading contact angle being lower at higher temperatures; this observation being well in agreement with previous studies carried out for tin droplets[20].

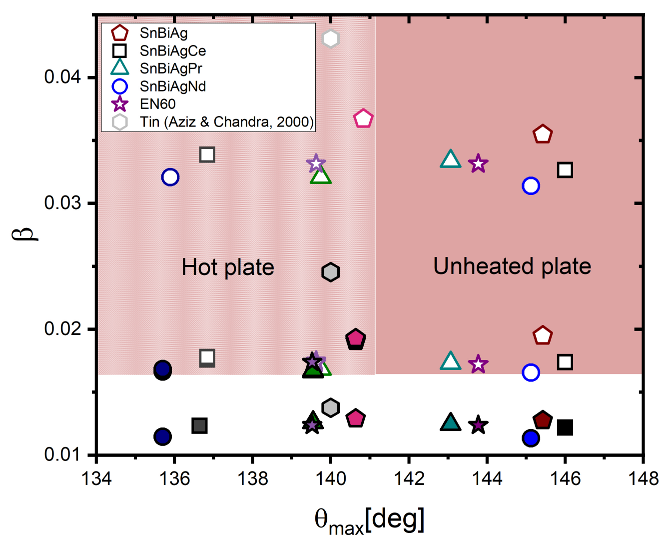

FIG. 6. The splashing ratio β in terms of the asymptotic spreading dynamic contact angle θ_{max}. Open symbols represent splashing while solid symbols stand for spreading or no splashing. All our experimental conditions are included here.

Molten solders and metallic alloys are unique among other fluids, for which their splashing behaviour is understood, owing to their significantly different liquid properties. For example, molten solders have densities approximately nine times higher than water, and surface tensions up to 30 times higher than ethanol. Interestingly, solder droplets spread at a contact angle of $\theta_{max} = 145 \pm 3$ degrees, which conforms to superhydrophobic dynamics[11]. A critical splashing ratio of $\beta \sim 0.0165$, seen in Figure 6, is significantly lower than that of water ($\beta \sim 0.060$) on hydrophobic substrates[11,19]. It is then not surprising that splashing is a common daily occurrence during electric soldering; millimetre-sized solder droplets splash on copper at significantly slower speeds than their water counterparts on wettable substrates; 1.15 ms versus 4.0 m/s.

IV. REMARKS

In this work, we have focused on experimental conditions closer to industrial interests, where the substrate is either at room temperature or at 220 Celsius. Our results show that the dynamic contact angle decreases with the substrate temperature, without affecting the critical splashing ratio. In addition, we have demonstrated that the splashing behaviour is successfully parameterised by the splashing ratio, a dimensionless scaling that includes the liquid properties and the air viscosity, and the maximum dynamic contact angle. This parametrisation is consistent among other liquids and substrates[19], and among the five different solders studied here. We have also shown that the fast-acting wetting dynamics of solders, e.g. the dynamic contact angle, at fast spreading speeds is also consistent with the spreading of other conventional liquids; molten solders/alloys acquires an asymptotic maximum contact angle value during spreading. We have also showed that rare-earth-dosed alloys present very similar wetting and splashing behaviour to that of commercial and undosed solders.

Surface effects are known to affect splashing. For example, Quetzeri et al. in 2019[19] demonstrated that surface roughness promotes splashing by increasing the maximum spreading contact angle. However, roughness also affects the splashing ratio by lowering the critical impacting speed. Future works could focus on extending our study to substrate temperatures beyond the melting point, or on studying the effect of flux on the wettability dynamics.

We end by noting that our results indicate that, in their current realisation, inkjet methods would not be suitable for the printing of solder alloys. Common commercial inkjet printers operate with droplet sizes of $D_0 = 50\ \mu$m at jetting speeds $U_0 > 5.0$ m/s, and these conditions result in a splashing ratio of $\beta \sim 0.0265$ which, according to our results, predicts splashing. In fact, a 50 μm solder droplet needs to impact a copper substrate at 3.8 m/s to spread without splashing.

SUPPLEMENTARY MATERIAL

Supplementary material is available, including the spreading dynamics of solder alloys on a heated copper plate, and a Table with equilibrium contact angles at various conditions.

AUTHOR'S CONTRIBUTIONS

Conceptualization: JRCP, JAdRP. Methodology: MAQS, JRCP, JAdRP Formal Analisis. KLMA, MAQS Funding Acquisition: JRCP, MANF Data Curation: KLMA, MAQS Validation: KLMA, JAdRP, MANF Writing/original draft preparation. MAQS, JRCP Writing Review & editing: JRCP. MAQS, JAdRP

ACKNOWLEDGMENTS

J.R.C.P. acknowledges the support from the UK Engineering and Physical Sciences Research Council through the project EP/V04382X/1. We would like to thank four anonymous reviewers for their thoughtful comments and efforts towards improving our manuscript.

DATA AVAILABILITY STATEMENT

AIP Publishing believes that all datasets underlying the conclusions of the paper should be available to readers. Authors are encouraged to deposit their datasets in publicly available repositories or present them in the main manuscript. All research articles must include a data availability statement stating where the data can be found. In this section, authors should add the respective statement from the chart below based on the availability of data in their paper.

AVAILABILITY OF DATA	STATEMENT OF DATA AVAILABILITY
Data available on request from the authors	The data that support the findings of this study are available from the corresponding author upon reasonable request.

REFERENCES

[1] V. Beedasy and P. J. Smith, "Printed electronics as prepared by inkjet printing," Materials **13**, 704 (2020).

[2] A. M. Worthington and R. S. Cole, "Iv. impact with a liquid surface studied by the aid of instantaneous photography. paper ii," Philosophical Transactions of the Royal Society of London. Series A, Containing Papers of a Mathematical or Physical Character **194**, 175–199 (1900).

[3] A. L. Yarin, "Drop impact dynamics: splashing, spreading, receding, bouncing...," Annu. Rev. Fluid Mech. **38**, 159–192 (2006).

[4]C. Josserand and S. T. Thoroddsen, "Drop impact on a solid surface," Annual review of fluid mechanics **48**, 365–391 (2016).

[5]C. Mundo, M. Sommerfeld, and C. Tropea, "Droplet-wall collisions: experimental studies of the deformation and breakup process," International journal of multiphase flow **21**, 151–173 (1995).

[6]S. Lin, B. Zhao, S. Zou, J. Guo, Z. Wei, and L. Chen, "Impact of viscous droplets on different wettable surfaces: Impact phenomena, the maximum spreading factor, spreading time and post-impact oscillation," Journal of colloid and interface science **516**, 86–97 (2018).

[7]C. Clanet, C. Béguin, D. Richard, and D. Quéré, "Maximal deformation of an impacting drop," Journal of Fluid Mechanics **517**, 199–208 (2004).

[8]C. Tang, M. Qin, X. Weng, X. Zhang, P. Zhang, J. Li, and Z. Huang, "Dynamics of droplet impact on solid surface with different roughness," International Journal of Multiphase Flow **96**, 56–69 (2017).

[9]S. Banitabaei and A. Amirfazli, "Droplet impact onto a solid sphere: Effect of wettability and impact velocity," Physics of Fluids **29**, 062111 (2017).

[10]H. Almohammadi and A. Amirfazli, "Droplet impact: Viscosity and wettability effects on splashing," Journal of colloid and interface science **553**, 22–30 (2019).

[11]M. A. Quetzeri-Santiago, K. Yokoi, A. A. Castrejón-Pita, and J. R. Castrejón-Pita, "Role of the dynamic contact angle on splashing," Physical review letters **122**, 228001 (2019).

[12]C. J. Howland, A. Antkowiak, J. R. Castrejón-Pita, S. D. Howison, J. M. Oliver, R. W. Style, and A. A. Castrejón-Pita, "It's harder to splash on soft solids," Physical review letters **117**, 184502 (2016).

[13]L. Xu, W. W. Zhang, and S. R. Nagel, "Drop splashing on a dry smooth surface," Physical review letters **94**, 184505 (2005).

[14]G. Riboux and J. M. Gordillo, "Experiments of drops impacting a smooth solid surface: a model of the critical impact speed for drop splashing," Physical review letters **113**, 024507 (2014).

[15]D. A. Burzynski and S. E. Bansmer, "Role of surrounding gas in the outcome of droplet splashing," Physical Review Fluids **4**, 073601 (2019).

[16]R. L. Vander Wal, G. M. Berger, and S. D. Mozes, "Droplets splashing upon films of the same fluid of various depths," Experiments in fluids **40**, 33–52 (2006).

[17]S. Faghiri, O. Mohammadi, H. Hosseininaveh, and M. B. Shafii, "The impingement of liquid boiling droplet onto a molten phase change material as a direct-contact solidification method," Thermal Science and Engineering Progress **23**, 100888 (2021).

[18]P. Poureslami, S. Faghiri, and M. B. Shafii, "Simultaneous double droplet impact on a molten phase change material pool: An experimental investigation," Physics of Fluids **35**, 027110 (2023), https://pubs.aip.org/aip/pof/article-pdf/doi/10.1063/5.0132570/16682535/027110_1_online.pdf.

[19]M. A. Quetzeri-Santiago, A. A. Castrejón-Pita, and J. R. Castrejón-Pita, "The effect of surface roughness on the contact line and splashing dynamics of impacting droplets," Scientific reports **9**, 1–10 (2019).

[20]S. D. Aziz and S. Chandra, "Impact, recoil and splashing of molten metal droplets," International journal of heat and mass transfer **43**, 2841–2857 (2000).

[21]M. V. Gielen, R. de Ruiter, R. B. Koldeweij, D. Lohse, J. H. Snoeijer, and H. Gelderblom, "Solidification of liquid metal drops during impact," Journal of fluid mechanics **883**, A32 (2020).

[22]R. Dhiman and S. Chandra, "Freezing-induced splashing during impact of molten metal droplets with high weber numbers," International journal of heat and mass transfer **48**, 5625–5638 (2005).

[23]S. Shakeri and S. Chandra, "Splashing of molten tin droplets on a rough steel surface," International Journal of Heat and Mass Transfer **45**, 4561–4575 (2002).

[24]D. Shen, G. Zou, L. Liu, W. W. Duley, and Y. N. Zhou, "Investigation of splashing phenomena during the impact of molten sub-micron gold droplets on solid surfaces," Soft Matter **12**, 295–301 (2016).

[25]M. Vaezi, H. Seitz, and S. Yang, "A review on 3d micro-additive manufacturing technologies," The International Journal of Advanced Manufacturing Technology **67**, 1721–1754 (2013).

[26]Q. Liu and M. Orme, "High precision solder droplet printing technology and the state-of-the-art," Journal of materials processing technology **115**, 271–283 (2001).

[27]D. Ii'yashchenko and S. Sapozhkov, "Splashing in manual arc coated electrode welding and methods of reducing splashing," Welding International **22**, 874–877 (2008).

[28]K.-K. Xu, L. Zhang, L.-L. Gao, N. Jiang, L. Zhang, and S.-J. Z. Zhong, "Review of microstructure and properties of low temperature lead-free solder in electronic packaging," Science and Technology of Advanced Materials **21**, 689–711 (2020).

[29]S. Hassam, E. Dichi, and B. Legendre, "Experimental equilibrium phase diagram of the ag-bi-sn system," Journal of Alloys and Compounds **268**, 199–206 (1988).

[30]V. Goodship, A. Stevels, and J. Huisman, *Waste Electrical and Electronic Equipment (WEEE) Handbook* (Woodhead Publishing, 2019).

[31]Z. Xia, Z. Chen, Y. Shi, N. Mu, and S. Na, "Effect of rare earth element additions on the

microstructure and mechanical properties of tin-silver-bismuth solder," Journal of Electronic Materials **31**, 564–567 (2002).

[32]Henkel Technologies, "Properties of alloys of multicore solder wires," https://stores.acrosales.com/content/solderwireproperties.pdf (2007), accessed 15-03-2023.

[33]A. Daerr and A. Mogne, "Pendent_drop: an imagej plugin to measure the surface tension from an image of a pendent drop," Journal of Open Research Software **4**, e3 (2016).

[34]J.-H. Chun, "The role of surface oxidation in the break-up of laminar liquid metal jets," Ph.D. dissertation, Massachusetts Institute of Technology (1996).

[35]W. Yang, R. Yang, Y. Yao, Z. Gao, and H. Zhang, "Effects of surface oxide layer on the impact dynamic behavior of molten aluminum droplets," Physics of Fluids (2023).

[36]Q. Xu, E. Brown, and H. M. Jaeger, "Impact dynamics of oxidized liquid metal drops," Physical Review E **87**, 043012 (2013).

[37]M. A. Quetzeri-Santiago, J. R. Castrejón-Pita, and A. A. Castrejón-Pita, "On the analysis of the contact angle for impacting droplets using a polynomial fitting approach," Experiments in Fluids **61**, 1–13 (2020).

[38]J. de Ruiter, D. Soto, and K. K. Varanasi, "Self-peeling of impacting droplets," Nature Physics **14**, 35–39 (2018).